

# Energy transfer and stimulated emission dynamics at 1.1 $\mu\text{m}$ in Nd-doped $\text{SiN}_x$

Rui Li,<sup>1</sup> Selçuk Yerci,<sup>1</sup> Sergei O. Kucheyev,<sup>2</sup> Tony van Buuren,<sup>2</sup> and Luca Dal Negro<sup>1,3,4,\*</sup>

<sup>1</sup>Department of Electrical and Computer Engineering, Boston University, 8 Saint Mary's Street, Boston, Massachusetts 02215 USA

<sup>2</sup>Lawrence Livermore National Laboratory, Livermore, California 94551 USA

<sup>3</sup>Division of Materials Science and Engineering, Boston University, 15 Saint Mary's Street, Brookline, Massachusetts 02446 USA

<sup>4</sup>Photonics Center, Boston University, 8 Saint Mary's Street, Boston, MA, 02215 USA

\*dalnegro@bu.edu

**Abstract:** Neodymium (Nd) doped amorphous silicon nitride films with various Si concentrations ( $\text{Nd:SiN}_x$ ) were fabricated by reactive magnetron co-sputtering followed by thermal annealing. The time dynamics of the energy transfer in  $\text{Nd:SiN}_x$  was investigated, a systematic optimization of its 1.1  $\mu\text{m}$  emission was performed, and the Nd excitation cross section in  $\text{SiN}_x$  was measured. An active  $\text{Nd:SiN}_x$  micro-disk resonator was fabricated and enhanced radiation rate at 1.1  $\mu\text{m}$  was demonstrated due to stimulated emission at the whispering gallery resonant modes. These results provide an alternative approach for the engineering of Si-based optical amplifiers and lasers on a silicon nitride materials platform.

©2011 Optical Society of America

**OCIS codes:** (230.5750) Resonators; (130.3120) Integrated optics devices; (160.5690) Rare-earth-doped materials; (140.3948) Microcavity devices; (140.5680) Rare earth and transition metal solid-state lasers.

---

## References and links

1. S. Yerci, R. Li, S. N. Basu, S. Kucheyev, A. Van Buuren, and L. Dal Negro, "Energy transfer and 1.54  $\mu\text{m}$  emission in amorphous silicon nitride films," *Appl. Phys. Lett.* **95**, 031107 (2009).
2. S. Yerci, R. Li, S. O. Kucheyev, A. Van Buuren, S. N. Basu, and L. Dal Negro, "Visible and 1.54  $\mu\text{m}$  emission from amorphous silicon nitride films by reactive cosputtering," *IEEE J. Sel. Top. Quantum Electron.* **16**(1), 114–123 (2010).
3. R. Li, S. Yerci, and L. Dal Negro, "Temperature dependence of the energy transfer from amorphous silicon nitride to Er ions," *Appl. Phys. Lett.* **95**(4), 041111 (2009).
4. A. Gopinath, S. V. Boriskina, S. Yerci, R. Li, and L. Dal Negro, "Enhancement of the 1.54  $\mu\text{m}$   $\text{Er}^{3+}$  emission from quasiperiodic plasmonic arrays," *Appl. Phys. Lett.* **96**(7), 071113 (2010).
5. T. J. Kippenberg, J. Kalkman, A. Polman, and K. J. Vahala, "Demonstration of an erbium-doped microdisk laser on a silicon chip," *Phys. Rev. A* **74**(5), 051802 (2006).
6. Y. Gong, M. Makarova, S. Yerci, R. Li, M. J. Stevens, B. Baek, S. W. Nam, R. H. Hadfield, S. N. Dorenbos, V. Zwiller, J. Vuckovic, and L. Dal Negro, "Linewidth narrowing and Purcell enhancement in photonic crystal cavities on an Er-doped silicon nitride platform," *Opt. Express* **18**(3), 2601–2612 (2010).
7. V. Lefèvre-Seguin, "Whispering-gallery mode lasers with doped silica microspheres," *Opt. Mater.* **11**(2-3), 153–165 (1999).
8. S. Yerci, R. Li, and L. Dal Negro, "Electroluminescence from Er-doped Si-rich silicon nitride light emitting diodes," *Appl. Phys. Lett.* **97**(8), 081109 (2010).
9. D. Olaosebikan, S. Yerci, A. Gondarenko, K. Preston, R. Li, L. Dal Negro, and M. Lipson, "Absorption bleaching by stimulated emission in erbium-doped silicon-rich silicon nitride waveguides," *Opt. Lett.* **36**(1), 4–6 (2011).
10. M. Lipson, "Guiding, modulating, and emitting light on silicon-challenges and opportunities," *J. Lightwave Technol.* **23**(12), 4222–4238 (2005).
11. D. Biggemann and L. R. Tessler, "Near infra-red photoluminescence of  $\text{Nd}^{3+}$  in hydrogenated amorphous silicon sub-nitrides  $\text{a-SiN}_x\text{:H<Nd>}$ ," *Mater. Sci. Eng. B* **105**(1–3), 188–191 (2003).
12. R. Li, J. R. Schneck, J. Warga, L. Ziegler, and L. Dal Negro, "Carrier dynamics and erbium sensitization in silicon-rich nitride nanocrystals," *Appl. Phys. Lett.* **93**(9), 091119 (2008).
13. R. D. Kekatpure and M. L. Brongersma, "Quantification of free-carrier absorption in silicon nanocrystals with an optical microcavity," *Nano Lett.* **8**(11), 3787–3793 (2008).
14. L. R. Doolittle, "Algorithms for the rapid simulation of Rutherford backscattering spectra," *Nucl. Instrum. Methods Phys. Res. B* **9**(3), 344–351 (1985).

15. M. J. F. Digonnet, *Rare-Earth-Doped Fiber Lasers and Amplifiers, Revised and Expanded* (CRC Press, 2001), pp. 43–71.
  16. P. C. Becker, N. A. Olsson, and J. R. Simpson, *Erbium-Doped Fiber Amplifiers—Fundamentals and Technology* (Academic, San Diego, 1999), pp. 87–129.
  17. D. Bréard, F. Gourbilleau, A. Belarouci, C. Dufour, and R. Rizk, “Nd<sup>3+</sup> photoluminescence study of Nd-doped Si-rich silica films obtained by reactive magnetron sputtering,” *J. Lumin.* **121**(2), 209–212 (2006).
  18. B. Redding, E. Marchena, T. Creazzo, S. Shi, and D. W. Prather, “Comparison of raised-microdisk whispering-gallery-mode characterization techniques,” *Opt. Lett.* **35**(7), 998–1000 (2010).
- 

## 1. Introduction

A major objective in silicon photonics research is the development of novel Si-compatible materials for the engineering of efficient light sources directly integrated on optical chips. Recently, erbium doping of silicon nitride films (Er:SiN<sub>x</sub>) has been proposed and investigated as a promising host platform characterized by efficient energy sensitization of Er emission, reduced free carrier losses at 1.54 μm [1–3], and compatibility with high quality photonic and plasmonic structures [4–7]. Moreover, based on the Er:SiN<sub>x</sub> materials platform, efficient electroluminescence, stimulated emission and pump-induced transparency of Er transitions at 1.54 μm have recently been demonstrated in electrical devices and high-quality nano-photon cavities, respectively [6–9]. However, as the development of Si-compatible light sources, micro-resonators, and low loss silicon nitride waveguides is steadily progressing [10], it is important to investigate alternative materials approaches capable of providing optical signals at shorter wavelengths within the wide transparency window of the active SiN<sub>x</sub> platform. Moreover, larger gain cross sections than the ones available by traditional erbium doping are also highly desirable. Based on these desiderations, we believe that neodymium (Nd) doping of silicon nitride structures could provide a potential solution for Si-based on-chip optical sources in the 1.1 μm spectral region. However, little is known on the radiative properties of Nd atoms embedded in the silicon nitride host matrix (Nd:SiN<sub>x</sub>), despite the 4-level energy structure of the 1.1 μm transition makes Nd ideally suited for the engineering of ultra low threshold lasers on a low-loss, silicon-compatible materials platform [11]. However, in order to fully leverage on this potential, it remains to be investigated if the Nd:SiN<sub>x</sub> materials approach can also benefit from reduced free carrier absorption at 1.1 μm, efficient energy sensitization of the optical emission, and enhanced stimulated emission rates compared to the more established Er:SiN<sub>x</sub> platform [12,13].

In this letter, we study the energy sensitization of the 1.1 μm Nd:SiN<sub>x</sub> photoluminescence (PL), its time dynamics and optimization in thin films fabricated by reactive magnetron sputtering in a large range of Nd and Si concentrations. Finally, we demonstrate enhanced radiation rate around 1.1 μm due to the coupling of stimulated emission with the resonant whispering gallery modes of an active Nd:SiN<sub>x</sub> micro-disk resonator.

## 2. Fabrication

### 2.1. Nd:SiN<sub>x</sub> films deposition

Nd:SiN<sub>x</sub> films were deposited at room temperature by N<sub>2</sub> reactive magnetron co-sputtering of Si and Nd targets in a Denton Discovery 18 confocal sputtering system. The relative concentration (at. %) of Si atoms in the sample was controlled between 44 and 49 by varying the N<sub>2</sub>/Ar flow ratio. The Si and Nd cathode powers and deposition pressure were kept constant for all samples. Post annealing process was performed in a rapid thermal annealing furnace at temperatures between 600 and 1150 °C for 200 s under forming gas (5% H<sub>2</sub>, 95% N<sub>2</sub>) atmosphere. The refractive indices and thicknesses of the samples were extracted by spectroscopic ellipsometry (A. J. Woollam VASE) using the Cauchy model. The atomic concentrations of Nd in the films were measured by Rutherford Back Scattering (RBS) assuming constant atomic density ( $9.53 \times 10^{22}$  atoms/cm<sup>3</sup>) and a layer composition of SiN<sub>x</sub>Nd<sub>y</sub> [14].

## 2.2. Nd:SiN<sub>x</sub> microdisk fabrication

A chromium mask was deposited after electron beam lithography to form circular patterns on the Nd:SiN<sub>x</sub> film defining the microdisk structure. Sulfur hexafluoride (SF<sub>6</sub>) and Ar gases were used to dry etch the Nd:SiN<sub>x</sub> and Tetramethylammonium Hydroxide (TMAH) was used to under etch the Si substrate underneath and to create the disk pedestal.

## 3. Experiment

### 3.1. Steady-state, time-resolved photoluminescence (PL) and PL excitation spectroscopy

The PL spectra of Nd:SiN<sub>x</sub> were excited at room temperature using a 458 nm line of an Ar ion laser (Spectra Physics, 177-602), which is non-resonant with the energy levels of Nd<sup>3+</sup> ions, and detected using an extended photomultiplier tube (Hamamatsu R5509-73). Figure 1 (a) shows a typical PL spectrum of Nd:SiN<sub>x</sub> obtained under steady state laser excitation. The spectrum features three main PL peaks corresponding to the three electronic radiative transitions of Nd<sup>3+</sup> ions. The inset of Fig. 1 schematically represents the Nd energy diagram for the relevant transitions investigated in this paper. We notice that despite the <sup>4</sup>F<sub>3/2</sub> – <sup>4</sup>I<sub>9/2</sub> transition centered on around 900 nm results in the strongest PL intensity, it is less interesting than the other two since it corresponds to the energetics of a three level system [15,16]. On the other hand, the <sup>4</sup>F<sub>3/2</sub> – <sup>4</sup>I<sub>13/2</sub> and <sup>4</sup>F<sub>3/2</sub> – <sup>4</sup>I<sub>11/2</sub> transitions provide a 4-level system recombination scheme and are therefore more appealing for the engineering of low threshold lasers.

In Fig. 1 (b) we provide direct evidence by PLE measurements of energy sensitization of the 1.1 μm Nd emission in a SiN<sub>x</sub> host matrix. A monochromatized Xe lamp was used as the light source for the photoluminescence excitation (PLE) experiments. All PLE spectra were intensity corrected by the spectrum of the Xe lamp and calibrated by the system response. In fact, we recall that a typical absorption spectrum for rare earth (RE) ions in the absence of energy sensitization from the host matrix should appear as a set of discrete peaks, corresponding to the inhomogeneous broadening of atomic RE levels. In particular, for the case of Nd two absorption peaks at 510 nm and 520 nm should be detected [15,16]. However, PLE spectra shown in Fig. 1 (b) do not reveal any well-defined peaks, which implies strong energy sensitization of Nd emission by the dielectric host matrix. Moreover, we observe in Fig. 1 (b) that the normalized PLE spectra red shift with the excess Si concentration in the films, following the modulation of the localized states of the SiN<sub>x</sub> band-tail absorption, analogously to what was shown for the 1.54 μm emission of Er:SiN<sub>x</sub> [1,2]. In Er:SiN<sub>x</sub> we recently demonstrated that the efficient energy transfer to Er ions originate from the coupling to the high density of localized states in the band-tails of the amorphous SiN<sub>x</sub> matrix [1,2]. Additionally, we showed that this type of energy transfer occurs on the nanosecond time scale [3].

We investigate the dynamics of energy transfer in Nd:SiN<sub>x</sub>. Time-resolved PL experiments in the visible spectral range (SiN<sub>x</sub> emission) were performed in Fig. 1(c) using a frequency doubled Ti:sapphire laser (Mai Tai HP, Spectra Physics) with 100 fs pulses at 430 nm and the emission was detected by a streak camera (Hamamatsu, C4770) with 10 ps time resolution. The energy transfer process leading to sensitization of the Nd emission can be considered as a non-radiative decay channel for the light-emitting SiN<sub>x</sub> matrix, driven by the Nd concentration. Figure 1 (c) indeed shows a pronounced decrease, on the nanosecond timescale, of the SiN<sub>x</sub> PL lifetime for samples with increasing Nd concentrations. By following the same steps of the analysis performed for Er:SiN<sub>x</sub> in Refs. [3,12], we can estimate from the data in Fig. 1 (c) an energy transfer time from SiN<sub>x</sub> to Nd ions in the range of 1 ~10 ns. This is of the same order of what we found for Er:SiN<sub>x</sub>, suggesting a similar nature for the energy transfer mechanism. In order to support further this interpretation, we measured the effective Nd excitation cross section (σ<sub>exc</sub>) in SiN<sub>x</sub> [1,2]. We used the PL system described above where we additionally modulated the laser pump beam using an acousto-optic modulator (Isomet, 1205C-2) and an oscilloscope yielding a system time response of about 10 μs. In Fig. 1 (d) we show a fit of our data using the well-known linear relation  $1/\tau_{on} = \sigma_{exc}\phi + 1/\tau_{Nd}$  connecting the pumping photon flux (φ) with the inverse of the PL decay (τ<sub>Nd</sub>)

and rise times ( $\tau_{on}$ ). The linear fit of our data resulted in  $\sigma_{exc} = 7.6 \times 10^{-17} \text{ cm}^2$ , which is very similar to the values measured for Er ions embedded in a  $\text{SiN}_x$  host matrix [1,2]. Additionally, given that the measured transfer times are comparable in both  $\text{Nd}:\text{SiN}_x$  and  $\text{Er}:\text{SiN}_x$  as discussed above, we conclude that the Nd emission can also be sensitized by the coupling with the localized bandtails states of the common  $\text{SiN}_x$  host matrix (It should also be noted that  $\text{Er}^{3+}$  and  $\text{Nd}^{3+}$  ions have similar bonding structures in the matrix) [1,2].

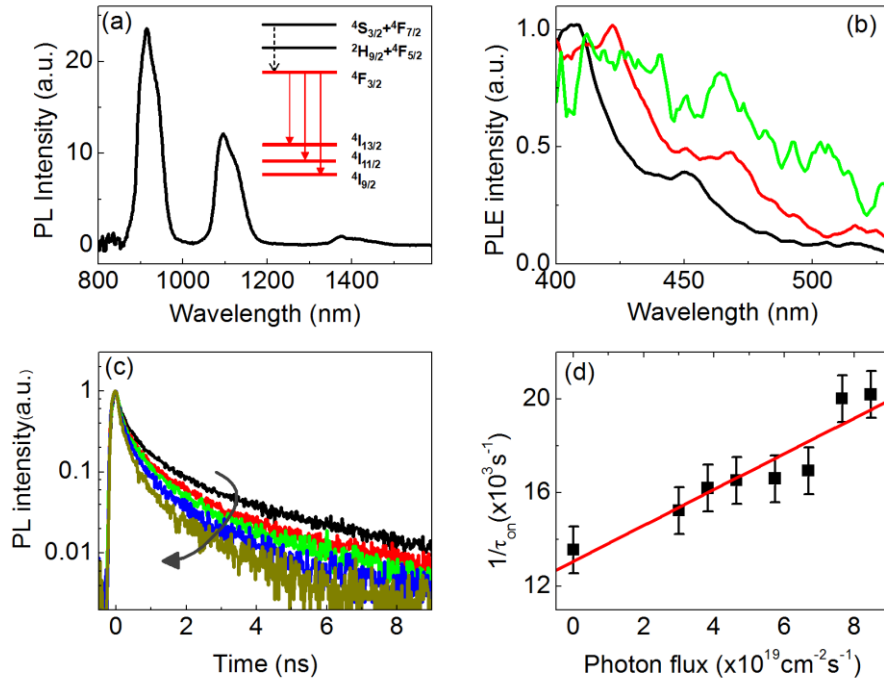


Fig. 1. (a)  $\text{Nd}:\text{SiN}_x$  PL spectrum of the sample with a Si at.% of 44 excited by a laser beam at 458 nm with a power of 1 mW. The inset shows an energy diagram of transitions in Nd ions. The red arrows indicate the observed transitions. The dashed arrow shows the nonradiative transitions. (b) Normalized PLE spectra with detection wavelength at 1100 nm for samples with refractive index of 2.13 (black), 2.16 (red) and 2.26 (green) corresponding Si concentrations of 45%, 47% and 49%, respectively. (c) Normalized PL decay traces at 600 nm for  $\text{Nd}:\text{SiN}_x$  samples fabricated with Nd target powers of 0, 8, 12, 18 and 22 W (increasing in the direction of the arrow). (d) The inverse rise time of the PL at 1.1  $\mu\text{m}$  excited at 458 nm with different excitation photon fluxes for a  $\text{Nd}:\text{SiN}_x$  with refractive index 2.13 (45% Si at.). All samples in (a), (b), (c) and (d) are annealed at 1000  $^\circ\text{C}$

### 3.2. Optimization of Nd emission in $\text{Nd}:\text{SiN}_x$

In Fig. 2 (a) we show the optimization of the 1.1  $\mu\text{m}$  Nd emission intensity in  $\text{Nd}:\text{SiN}_x$  with respect to deposition and materials parameters. To optimize the PL intensity and emission lifetime, the Nd concentration (Fig. 2 (a)), the annealing temperature (Fig. 2 (b)) and excess Si concentration (Fig. 2 (c)) were varied. For that purpose, we fabricated  $\text{Nd}:\text{SiN}_x$  samples with varying Nd concentrations and the same Si concentration of 44 at.% (as optimized in Fig. 2 (c)). Stronger PL intensity and longer lifetimes are desirable to achieve high efficiency of the  $\text{Nd}:\text{SiN}_x$  emission. In order to compare the lifetime data of different samples, we have defined an effective PL lifetime as  $\tau_{eff} = (A_1 \times t_1 + A_2 \times t_2)/(A_1 + A_2)$ . This choice is due to the strongly non-exponential nature of the Nd lifetime shown in the inset of Fig. 2 (b) for a representative sample [17]. For all the samples, the PL decay trace can be fitted by a two-exponential decay model. The fitting parameters for the data in the inset of Fig. 1 (b) are  $\tau_1 =$

50  $\mu\text{s}$  and  $\tau_2 = 140 \mu\text{s}$  with respective amplitudes (branching ratios) of  $A_1 = 0.53$  and  $A_2 = 0.47$ .

As shown in Fig. 2 (a), the Nd:SiN<sub>x</sub> effective PL lifetime at 1.1  $\mu\text{m}$  decreases with Nd target power due to concentration quenching and the 1.1  $\mu\text{m}$  PL intensity is optimized with Nd concentrations of the order of  $10^{20} \text{cm}^{-3}$ , which is similar to the case of Nd doped glasses [15]. Figure 2 (b) and (c) summarize the evolution of the PL emission lifetime for different annealing temperatures and excess Si concentrations, respectively. Moreover, Fig. 2 (d) shows the optimization of the PL intensity with annealing temperature. We found that both PL intensity and lifetime are optimized at 1000  $^\circ\text{C}$ . At higher temperatures, intrinsic defects states due to Si and Nd segregation could form in the matrix deteriorating the local environment of Nd ions and reducing the PL efficiency, as shown in Er:SiN<sub>x</sub> films [1,2]. Moreover, we found that both PL intensity and lifetime of Nd:SiN<sub>x</sub> decrease dramatically by increasing the excess Si concentration. Since the optical gap of the amorphous SiN<sub>x</sub> matrix decreases with excess Si concentration [2], we expect that an increased density of localized defect states in the matrix will couple to the  $^4F_{3/2}$  Nd excited state and deteriorate its emission rate and PL intensity due to non-radiative recombinations. In summary, our optimization study shown in Fig. 2 has led us to conclude that the evolution of PL intensity and lifetime with excess Si, annealing temperature and Nd concentration for Nd:SiN<sub>x</sub> is similar to Er:SiN<sub>x</sub>, except that Nd ions are subjected to more efficient non-radiative recombinations due to the higher energy of the excited state. However, the unique advantages of the 1.1  $\mu\text{m}$  Nd emission with respect to the Er one is related to its four-level system energetics and to a larger stimulated emission cross section [15,16]. In order to demonstrate this point, we have fabricated an optimized Nd:SiN<sub>x</sub> micro-disk resonator and investigated its time dynamics around the 1.1  $\mu\text{m}$  emission band.

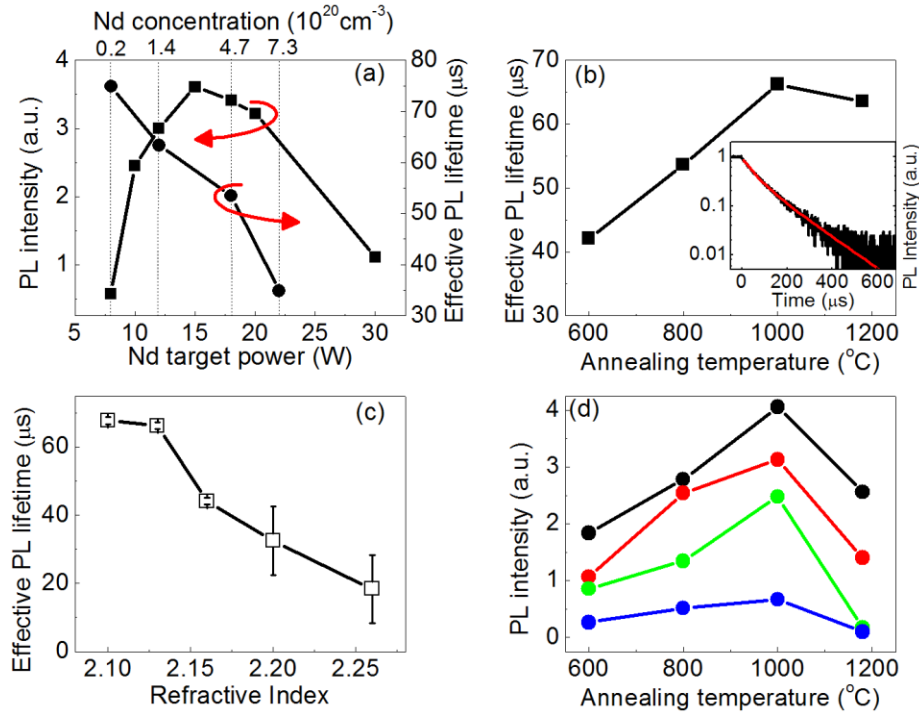


Fig. 2. (a) Nd:SiN<sub>x</sub> PL intensity and effective PL lifetime at 1100 nm for samples (~280 nm thick) with different Nd concentrations (Nd target powers) and annealed at 1000  $^\circ\text{C}$ . Nd:SiN<sub>x</sub> effective PL lifetime at 1100 nm for samples (~800 nm thick) with (b) annealing temperatures of 600, 800, 1000 and 1180  $^\circ\text{C}$  (Inset: A representative decay trace of Nd:SiN<sub>x</sub> PL at 1100 nm, fitted by a two-exponential decay model) and (c) refractive indices of 2.11, 2.13, 2.16, 2.20 and 2.26 (corresponding Si concentrations of 44, 45, 47, 48 and 49%). (d) Nd:SiN<sub>x</sub> PL intensity at 1100 nm for samples with annealing temperatures of 600, 800, 1000 and 1180  $^\circ\text{C}$  and different Si concentrations (45% black, 47% red, 48% green and 49% blue).

### 3.3. Stimulated emission from Nd:SiN<sub>x</sub> microdisk

Figure 3 (a) shows a scanning electron micrographs image of the fabricated active Nd:SiN<sub>x</sub> microdisk with 9.8 μm in diameter deposited using 15W Nd cathode power and subsequently annealed at 1000 °C. The sidewall roughness limits the quality factor of the resonant modes to approximately  $5 \times 10^4$  (data not shown here). To characterize the emission dynamics from the resonant whispering gallery modes, the entire micro-disk was excited from the top by an Ar ion laser focused using a 50X objective. The sample is excited using all the lines (458, 488 and 514 nm) of our Ar ion laser in order to increase the pumping efficiency. It should be noticed from the PLE spectra in Fig. 1(b) that the excitation of the Nd ions occurs indirectly through the SiN<sub>x</sub> matrix for all the considered wavelengths. Since the modes with relatively low Q factor radiate more easily to the far field, we could collect them by a lens focused on the disk edge [13,17,18]. The inset of Fig. 3 (b) shows low Q whispering gallery modes collected in emission from the Nd:SiN<sub>x</sub> micro-disk. We measured the PL lifetime of the Nd:SiN<sub>x</sub> micro-disk at the resonant wavelengths of 1083 nm, 1101 nm and 1120 nm (downward arrows in Fig. 3 (b) inset) as well as at the non-resonant wavelengths at 1190 nm, 1108 nm and 1136 nm (upward arrows in Fig. 3 (b) inset). Our data in Fig. 3 (b) shows that, despite the limitations of low Q disk modes, the PL decay dynamics collected at the resonant wavelengths is consistently faster than the one collected for non-resonant modes of neighboring wavelengths.

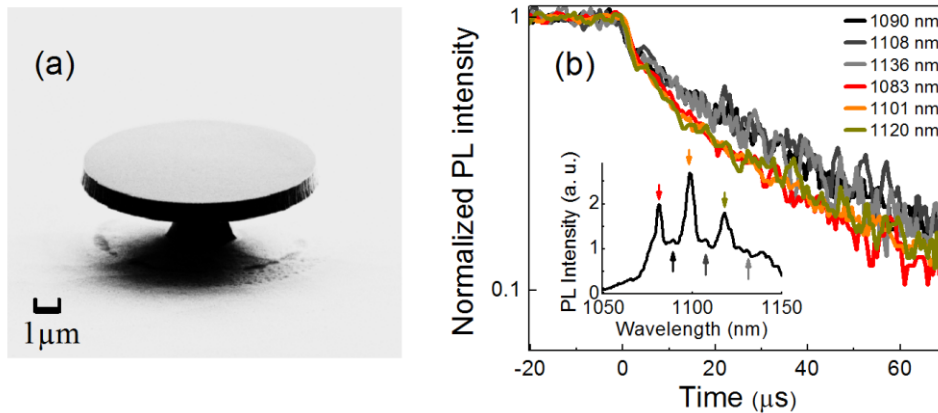


Fig. 3. (a) SEM image of a Nd:SiN<sub>x</sub> microdisk with a diameter of 9.8 μm. (b) PL decay traces of the Nd:SiN<sub>x</sub> microdisk centered at different wavelengths as indicated in the legend. Inset: PL spectrum of the Nd:SiN<sub>x</sub> microdisk (colors of the arrows indicates the colors of the corresponding PL decay traces).

In principle, several factors could cause lifetime shortening in a micro-disk, such as higher non-radiative recombination rates due to strong excitation, excited state absorption in the material, radiative Purcell effect and the onset of stimulated emission. Of all these different factors, we believe that only stimulated emission can be responsible for the observed PL lifetime shortening under our experimental conditions. In fact, the PL from the non-resonant modes is collected under identical pumping conditions and therefore the pump-induced non-radiative recombinations plays an identical role for both on and off-resonance modes. Next, the shorter lifetimes could originate from the stronger signal (PL) intensity at the resonant wavelengths due to excited state absorption, where the electrons at the Nd excited state could absorb signal (PL) photons and get promoted to a higher lying energy state at an energy equal to the difference between the  $^4F_{3/2}$  and the  $^4I_{11/2}$  levels. However, such an upper energy state does not exist within the Nd energy manifold. The Purcell effect has been shown to shorten the lifetime at the resonant wavelength around 1.5 μm in Er:SiN<sub>x</sub> photonic nanocavities [6]. However, due to the much larger modal volume and the low Q factor of the investigated modes, we expect the Purcell enhancement in our micro-disk to be negligible. The observed

on-resonant lifetime shortening can be attributed to the onset of stimulated emission in the disk. In fact, the 4-level system in Nd ions enables population inversion with no absorption threshold and Nd ions have a larger stimulated emission cross section than Er [15]. These two factors make lifetime shortening easier to observe in Nd resonant cavities compared to Er-doped ones. However, despite our demonstration of stimulated emission in the system, the pump power dependence of the PL at the cavity modes still exhibits a sub-linear trend (data not shown here), implying that we have not yet achieved the micro-disk lasing regime due to the large sidewall roughness losses which limit the Q-factor of the disk. However, the observation of stimulated emission in Nd:SiN<sub>x</sub> shows great promises for the engineering of on-chip lasers based on this novel materials platform.

#### **4. Conclusions**

In summary, Nd:SiN<sub>x</sub> materials were fabricated and optimized in terms of PL intensity and emission lifetime. Similar to the case of Er:SiN<sub>x</sub>, nanosecond-fast energy transfer from localized states in the bandgap of SiN<sub>x</sub> to Nd ions was observed and the role of excess Si and Nd concentration in these films discussed. The effective Nd excitation cross section for the 4-level 1.1 μm transition was measured and an active Nd:SiN<sub>x</sub> micro-disk was fabricated. Stimulated emission from the resonant modes of the disk was demonstrated under optical pumping. These results show that the Nd:SiN<sub>x</sub> materials platform bears great promises for the fabrication of Si-based laser.

#### **Acknowledgments**

This work was partially supported by the AFOSR under MURI Award No. FA9550-06-1-0470 on “Electrically-Pumped Silicon-Based Lasers for Chip-Scale Nanophotonic Systems” supervised by Dr. Gernot Pomrenke and by the NSF Career Award ECCS-0846651. Work at LLNL was performed under the auspices of the U.S. DOE by LLNL under Contract DE-AC52-07NA27344.